Experimental Investigations on the Strength and Serviceability of Biaxial Hollow Concrete Slabs

Oukaili, Nazar
Professor
College of Engineering-University of Baghdad
dr_nazar12000@yahoo.com

Hassan Hamoudi Yasseen
Lecturer
College of Engineering-University of Baghdad
hassanbayati@ymail.com

ABSTRACT

Biaxial hollow slab is a reinforced concrete slab system with a grid of internal spherical voids included to reduce the self-weight. This paper presents an experimental study of behavior of one-way prestressed concrete bubbled slabs. Twelve full-scale one-way concrete slabs of (3000mm) length with rectangular cross-sectional area of (460mm) width and (150mm) depth. Different parameters like type of specimen (solid or bubbled slabs), type of reinforcement (normal or prestress), range of PPR and diameter of plastic spheres (100 or 120mm) are considered. Due to the using of prestressing force in bubbled slabs (with ratio of plastic sphere diameter D to slab thickness H, D/H=0.67), the specimens showed an increase in ultimate load capacity ranging between (79.3% and 125%) and a decrease in the deflection at service load of about (9.8% to 12%) with respect to the control bubbled reinforced concrete slab. Also, it is found that, the bubbled slabs have about (79% to 86%) of the ultimate load capacity of a similar reference solid slab. At the same time the influence of voids present in the bubbled slabs is reflected in a decrease in the first cracking load by about (14.8% to 29.6%) in comparison with solid slabs.

Key words: one way slabs, bubbled slabs, spherical voids, prestressed concrete, shear failure.

تحريات عملية على مقاومة وصلاحية التشغيل للبلاطات الخرسانية المجوفة بمحورين

نزار كامل علي العقيلي
جامعة بغداد- كلية الهندسة
استاذ

حسن حمودي ياسين
جامعة بغداد- كلية الهندسة
مدرس

الخلاصة

البلاطات المجوفة هي بلاطة خرسانية لَها ترتيب ثنائي الأبعاد من الفراغات لغرض تَخفيض الوزنِ الذاتي.تقدم هذه الدراسة تحري عملي على سلوك البلاطات الخرسانية احادية الاتجاه والمسبقة الشد ذات الفراغات البلاستيكية الكروية. اجريت الدراسة على اثني عشر بلاطة احادية الاتجاه بابعاد (3000 ملم) طولا وذات مقطع مستطيل بابعاد (460 ملم) عرضا و (150 ملم) ارتفاعا. اخذت بنظر الاعتبار المتغيرات الاساسية مثل نوع البلاطات الخرسانية (بلاطات صلبة او مجوفة)و نوع التسليح وقطر الكرات البلاستيكية المجوفة (100 ملم او 120 ملم). نتيجة لاستخدام تسليح الشد المسبق الجهد في البلاطات المجوفة (التي فيها نسبة قطر الكرة الى سمك البلاطة مساويا الى 0.67) تزايدت السعة الحملية لتصل (79.3% الى 125%) في حين ان الهطول عند الحمل الخدمي انخفض بنسبة (9.8% الى 12%)، على التوالي، مقارنة مع البلاطه المجوفة ذات التسليح الاعتيادي. اظهرت النتائج بان الحمل الاقصى للبلاطات المجوفة يساوي نسبة (79% الى 86%) من الحمل الاقصى لنضيراتها الصلدة. في نفس الوقت، نتيجة لوجود الفراغات في البلاطات المجوفة لوحظ انخفاض في الحمل المسبب للتشقق بمقدار (14.8 % الى 29.6%).

الكلمات الرئيسية: البلاطات ذات الاتجاه الواحد، البلاطات المتفقعة، الفراغات الكروية، الخرسانة مسبقة الشد، فشل القص.

1. INTRODUCTION

Various attempts have been made in the past to reduce the weight of concrete slabs, without reducing their flexural strength. Not all the internal concrete can be replaced though, since aggregate interlock of the concrete is important for shear resistance, concrete in the top region of the slab is necessary to form the compression block for flexural resistance, and concrete in the tension zone of the slab needs to bond with reinforcement to make the reinforcement effective for flexural resistance. Also the top and bottom faces of the slab need to be connected to work as a unit and insure the transfer of the stresses, **Marais, 2009**. The dominant advantage of slabs with internal spherical voids is that it uses (35 %) less concrete than normal solid slabs. The plastic spheres replace the non-effective concrete in the centre of the section, thus reducing the dead load of the structure by removing unused heavy material which leads to less structural steel since the need for reinforcement diminishes. Accordingly, the building foundations are designed for smaller dead loads as well. On site, construction time can be shortened since slabs with internal spherical voids can be precast, in relation to savings in material and time; cost reductions are also typical with this system as shown in **Fig. 1**. Sustainable analysis gives a fact that the energy consumption and CO_2 emission can be reduced by about (30% to 50%), **BubbleDeck, Lighter Flat, 2006**. Studies and tests have shown that bubbled deck has approximately (87%) of the flexural stiffness of a solid slab. If no other measures were taken, this would mean marginally higher deflections at serviceability limit state than in an equivalent solid slab in direct proportion to this ratio, **BubbleDeck, Technical Paper, 2006**.

The Eindhoven University, performed test on the bending stiffness of bubbled slabs by focusing on the smallest and largest depths of the available slabs, (230 and 450mm). They found that the flexural behavior of bubbled slab is the same as a solid slab, practically and theoretically. Also, the Technical University of Darmstadt, performed tests on the stiffness of a bubbled deck slab, the results verified with the theoretical analysis and with the physical tests done in the Netherlands. For the same strength, bubbled deck has (87%) of the bending stiffness of a similar solid slab but only (66%) of the concrete volume due to the bubbles was used, therefore, the typical deflection was marginally higher than that of a solid slab, as expected, **BubbleDeck, Test and Report, 2006**. **Salman, 2012**, studied the flexural capacities of reinforced concrete two-way hollow slabs with plastic sphere voids, fifteen reinforced concrete square slabs of (1000mmx1000mm) have tested. It has been found that bubbled slab, (with ratio of bubble diameter B to slab thickness H, B/H=0.80), has about (90 to 100%) of the ultimate load capacity of a similar solid slab. Shear strength of any concrete slab is chiefly dependent on the effective mass of concrete. Due to the inclusion of plastic bubbles, the shear resistance of a bubbled deck slab is greatly reduced compared to a solid slab. From theoretical models, the shear strength of the voided slab was determined to be (60-80%) of a solid slab with the same depth. Therefore, a reduction factor of (0.6) is to be applied to the shear capacity of all bubbled deck slabs, **BubbleDeck, Technical Paper, 2006**. **Nielsen, 2006**, investigated both the shear strength and punching shear resistance for a slab of a depth of (188mm), which is not a typical bubbled deck thickness, and used an (a/d) ratio of (1.4). It is found that shear strength was approximately (80%) of a solid slab, and that punching shear was (90%) of the same slab.

2. CONCEPT OF PARTIAL PRESTRESSING RATIO

The partial prestressing ratio (PPR) was proposed by **Naaman 1992** to quantify the amount of prestress in a partially prestressed beam. It is defined as the ratio of the nominal moment resistance provided by the prestressing steel, M_{up}, to the total nominal moment

resistance of the member, M_{up+s}, **Naaman, 1992**:

$$PPR = \frac{M_{up}}{M_{up+s}} = \frac{A_{ps} f_{py}(d_p - \frac{a}{2})}{A_{ps} f_{py}(d_p - \frac{a}{2}) + A_s f_y(d - \frac{a}{2})} \quad \text{Eq. (1)}$$

For the fully prestressed concrete (A_s = 0), the value of PPR equals (1), and for the partially prestressed concrete, this value will be less than (1). It is observed that, in the range of PPR between (40%) and (70%), partially prestressed concrete beams have capacities to behave in ductile manners, **Karayannis, 2013**.

3. EXPERIMENTAL PROGRAM

Twelve full-scale one-way structural concrete slabs of (3000mm) length with rectangular cross-sectional area of (460mm) width and (150mm) depth were tested as simply supported under two line load system. Load (P) is applied by means of hydraulic jack which acted on the slabs as two symmetrical concentrated loads (with ratio of shear span (a) to effective depth (d), a/d=6.88) (see **Fig. 2**). The twelve slabs were divided into three groups according to the main variables as shown in **Table 1**. Group 1, includes three solid slabs (S1 to S3), without plastic spheres as shown in **Fig. 3**. Group 2, includes six bubbled slabs (BD1 to BD6), in which each specimen contain (80) plastic sphere voids of (100mm) diameter with a reduction in self-weight of (26.4%) and a sphere diameter to slab depth ratio of (0.67) as shown in **Fig. 4**. Group 3, includes three bubbled slabs (BD7 to BD9), in which each specimen contain (48) plastic sphere voids of (120mm) diameter with a reduction in self-weight of (27.36%) and a sphere diameter to slab depth ratio of (0.80) (see **Fig. 5**).

The test parameters studied were the type of slab specimen (solid or bubbled), diameter of plastic sphere and the partially prestressing ratio (PPR), which varied between (0.0 and 1.0). The specimens were constructed using a concrete with a compressive strength of approximately (40 MPa). The water/cement ratio of (0.4) fits with the strength required. The mixing proportion (water, cement, sand, coarse aggregate and super plasticiser) is (178, 445, 532, 1240 and 9.9kg/m^3), respectively. Seven-wire strand of (12.7 mm) nominal diameter (grade 270, low relaxation, confirming to **ASTM A416/ A416M-06**) used as flexural reinforcement, at a prestressing level of (70%) of the ultimate strength (1860 MPa). The relation between the load and the elongation is shown in **Fig. 6**. In addition, different diameters (12mm, 10mm and 6mm) of steel bars used in this study as flexural and shear reinforcement. The plastic spheres, (hollow balls), made by recycled plastic with diameters of (100 mm and 120 mm).

Distribution and fixing of the plastic spheres inside the reinforcement cage of the bubbledeck slab is achieved by upper and lower (50x50) welded wire meshes of (3mm) diameter. Steel stirrups of (6mm) diameter were used to fix the upper and lower meshes in the required position. The support region is designed to be solid, (without plastic spheres), at distance (350mm) from the end of the member to increase the shear strength of the slab, also steel bars of (12 mm and 10 mm) diameter were used as tension and compression reinforcement, respectively, as shown in **Fig. 7**. After the preparation of the reinforcement cage it is inserted in the mould at the prestressing bed. The strands are jacked to a load of (140 kN) (0.7*fpu*) each one individually. The fresh concrete is poured into the moulds and compacted. The prestressing force

is transferred to the slab by cutting the strand after (7) days of casting when the required compressive strength of concrete has been reached.

4. TEST RESULTS AND DISCUSSION

4.1 Load-Deflection Response

Deflection was measured at the midspan of tested slabs by means of (0.01mm) dial gauge as shown in **Fig. 8**. The behavior of the solid and bubbled slab specimens with different partial prestressing ratio was studied at two load stages: the service load and the failure load stages. The serviceability load limit consists about (70% - 75%) of the failure load, **Tan and Zhao, 2004**.

The test results of deflection at first cracking, service and failure loads were presented in **Table 2**. In general, the presence of plastic spheres in the bubbled slab reduces its stiffness. Accordingly, the plastic sphere voids, which used in the bubbled slabs (BD1 to BD3) and (BD7 to BD9), increase the deflection at the same stage of loading in comparison with reference solid slabs (S1 to S3), respectively, because the spherical voids decreased the flexural rigidity of bubbled slabs. For bubbled slab (BD1), where (PPR=0.0), the deflection at ultimate service load equal to (7.6 mm), while for (BD2 and BD3), where (PPR=0.74 and 1.0), the deflection at ultimate service load equal to (9.6 mm and 6.85 mm), respectively. Also, at the same stage of loading, the effect of using prestressing steel in bubbled slabs (BD2 to BD3), significantly decreased the deflection compared to the bubbled slabs (BD1). It is noted that, the measured camber for bubbled slab (BD2) with (PPR=0.74) is (6%) smaller than that of bubbled slab (BD3) with (PPR=1), as shown in **Fig. 9**.

It is observed that, decreasing the partial prestressing ratio to be (0.52) rather than (0.74) by increasing the number of ordinary steel bar of (12mm) diameter from (2) to (6) in bubbled slab (BD4), decreases the camber by about (6.1%) in comparison with bubbled slab (BD2), as shown in **Table 2**. Also, the influence of decreasing the (PPR) in the bubbled slab (DB4), decreases the deflection at ($0.7P_u$) by about (1.14%), while, the ultimate deflection increases by about (7.7%) compared to the bubbled slab (BD2).

The test results show that, increasing the partial prestressing ratio to be (0.81) rather than (0.74) by increasing the number of prestressed strands from (2) to (3) in bubbled slab (BD5), increases the camber by about (73%) in comparison with bubbled slab (BD2). Also, increasing the number of strand in bubbled slabs (BD5 and BD6) with (PPR=0.81 and 1.0), decreases the deflection at ($0.7P_u$) and the ultimate deflection. The percentage of the decreasing of the deflection at ($0.7P_u$) reaches (21% and 36.3%), respectively. The percentage of the decreasing of ultimate deflection reaches (3% and 9%), respectively, in comparison with the bubbled slabs (BD2and BD3), respectively.

It is observed that, there is a significant increase in the recorded deflection at service load ($0.7P_u$) for bubbled slab (BD5) with (PPR=0.81) about (73.8%) over the bubbled slab (BD6) with (PPR=1), while, at failure this percentage becomes (33%).

Using plastic spheres with (120mm) diameter in bubbled slabs (BD8 and BD9), increases the camber by about (12% and 11%) compared to the bubbled slabs (BD2 and BD3), respectively, as shown in **Table 2**. Also, the influence of increasing the diameter of plastic spheres used in bubbled slabs (BD7, BD8 and BD9), increases the deflection at ($0.7P_u$) and

ultimate deflection. The percentage of the increased deflection at ($0.7P_u$) reaches (29.7%, 0.5% and 25.2%) and the percentage of the increased ultimate deflection reaches (2%, 10% and 10.1%) over the bubbled slabs (BD1, BD2 and BD3), respectively

4.2 First Cracking and Ultimate Load Results

The test results showed that, due to the existence of a grid of voids in bubbled slab specimens, the first cracking, the ultimate service and the failure loads decreased in comparison with the reference solid slabs. The bubbled slabs with different PPR values had about (82% to 85%) of the failure load capacity of a similar reference solid slabs. In comparison with the bubbled slabs (BD1), where (PPR=0.0), using prestressing steel in the bubbled slabs (BD2 and BD3), where (PPR=0.74 and PPR=1.0) respectively, significantly increased the first cracking, the ultimate service and the failure loads. That depends on the PPR value (see **Table 2**). The increase of the first cracking load for bubbled slabs (BD2 and BD3) attained (228% and 185.7%), respectively, while the increase of the failure load reached (97.7% and 79.3%), respectively.

For bubbled slab (BD2), where (PPR=0.74), the first cracking and ultimate loads equal to (46kN and 86kN), respectively, while for (BD4), where (PPR=0.52), the first cracking and ultimate loads reached (54kN and 92kN), respectively.

Increasing the number of strand in bubbled slabs (BD5 and BD6) with (PPR=0.81 and 1.0), respectively, increase the first cracking and ultimate loads. The percentage of the increasing of the first cracking load reaches (41.3% and 52.5%), and the percentage of the increasing of the ultimate load reaches (13.9% and 20.5%) in comparison with the bubbled slabs (BD2 and BD3), respectively, as shown in **Table 2**.

It can be seen that, there is a small increase in the first crack and ultimate loads for bubbled slab (BD5) with (PPR=0.81) by about (6.5% and 4.2%), respectively, in comparison with the bubbled slab (BD6) with (PPR=1).

The influence of increasing the diameter of plastic spheres used in bubbled slabs (BD7, BD8 and BD9), decreases the first cracking load by about (14.2%, 17.4% and 25%) in comparison with bubbled slabs (BD1, BD2 and BD3), respectively, but at failure this percentage become (3.4%, 4.6% and 7%), respectively. Also, in the case of (PPR=1) in the bubbled slab (BD9), using fully prestressed reinforcement increases the first cracking load by about (150%), while, the ultimate load increases by about (72.6%) in comparison with bubbled slab (BD7). For bubbled slab (BD8), where (PPR=0.74), the first cracking and ultimate loads increased by (26.6% and 13.1%), respectively, compared with the bubbled slab (BD9).

4.3 Load-Concrete Normal Strain Relationship

Concrete normal strains are measured using demec discs which were placed on the compression, central and tension faces of the slab in horizontal direction. The position and direction of the demec discs are shown in **Fig. 8**. For prestressed slabs, when the eccentric prestressing force is transferred to the concrete through the bond, instantaneous losses of prestressing force occur due to elastic shortening of the concrete. The change in strain in the prestressing steel is approximately equal to the normal compressive strain in the concrete at the

steel level. The initial concrete strains at midspan due to effective prestressing force which is calculated by elastic theory on the basis of a transformed section, taking into consideration the area of steel are added to the concrete strains which is measured by demec discs. **Figs. 10** to **20** represent the variation of normal strain over the depth of cross-sections due to incremental loads for tested slabs in flexural span.

The plastic voids are positioned in the middle of cross section of the bubbled slabs, where concrete has limited effect maintaining solid sections in top and bottom where high stresses can exist. Therefore, the plastic sphere voids, which exist in the bubbled slabs (BD1 to BD3) and (BD7 to BD9), increase the concrete strain at the same stage of loading in comparison with the reference solid slabs (S1 to S3). Using of prestressing steel in slabs (BD2 and BD3), where (PPR=0.74 and PPR=1), respectively, give a large decrease in the concrete strains, in comparison with the bubbled slabs (BD1), where (PPR=0.0) as shown in **Figs. 14** and **15**.

Also, decreasing the partial prestressing ratio to be (0.52) rather than (0.74) in the bubbled slab (DB4), decrease the maximum concrete compressive and tensile strains at midspan compared to the bubbled slab (BD2) (see **Fig. 16**).

The test results show that, increasing the number of strands in bubbled slabs (BD5 and BD6), decrease the maximum concrete compressive and tensile strains, in comparison with the bubbled slabs (BD2and BD3), respectively.

The effect of increasing the diameter of plastic spheres, used in bubbled slabs (BD7, BD8 and BD9), increases the concrete compressive and tensile strains compared to the bubbled slab (BD1, BD2 and BD3), respectively. This is due to the thin concrete cover in the compression and tension zones. Also, there is a significant decrease in concrete strains for bubbled slab (BD8 and BD9) with (PPR=0.74 and 1), respectively, compared with the bubbled slab (BD8) with (PPR=0).

4.4 Crack Pattern and Failure Mode

The test results of the maximum crack width, number of cracks, shear failure angle and mode of failure for tested slabs were presented in **Table 3**. The effect of plastic spheres causing voids in bubbled slabs, and the cracks will translate in a sudden propagation from solid to void zone forming an increase in crack width and a decrease in number of cracks in comparison with the solid slabs. There is a significant decrease in the maximum crack width and the number of cracks for bubbled slab with fully and partially prestressed reinforcement in comparison with non-prestressed bubbled slabs.

For bubbled slab (BD2), where (PPR=0.74), the maximum crack width equals to (0.27mm), while for (BD4 and BD5), where (PPR=0.52 and 0.81), the maximum crack width equals to (0.21 mm and 0.22 mm), respectively, as shown in **Table 3**.

Flexural cracks appeared at the soffit of the concrete slabs whenever the tensile stresses exceeded the modulus of rupture of concrete. Further development of flexural cracks occurred parallel to these cracks and slowly propagated throughout the thickness of the slab, on increasing the application of load, greater deflections occur at the slab midspan. Flexural-shear cracks form as the slab approaches failure as shown in **Figs. 2**1, **24** and **30**. Slabs (S1, BD1 and BD7) showed flexural failure mode by yielding of the steel in tension zone, while slab (S2) failed in

flexural due to concrete crushing at the top fibers as shown in **Fig. 22**.

Shear failure mode with two types of shear cracks were observed in prestressed slabs (S3, BD2 BD3, BD4, BD5, BD6, BD8 and BD9). These cracks are as follow:

1-Web-shear cracks, which initiate in the region occupied by the plastic spheres (voided section) of the bubbled slabs (BD2, BD4, BD5, BD6 and BD8), when the principal tensile stress in the concrete exceeded its tensile strength, a sudden opening of an explosive destructive diagonal tension crack may take place in the voided section. This extends to a distance from the support section to the load point section and results in the destruction of the bond between the concrete and steel leading to immediate collapse of the bubbled slab in a web-shear failure mode as shown in **Figs. 25, 27, 28, 29** and **31**.

2-Flexural-shear cracks, occur after flexural cracking has taken place. The flexural crack extends more vertically into the slabs (S3, BD3 and BD9) from the tension face. When a critical combination of flexural and shear stresses develops at the tip of the flexural crack, that crack propagates in an inclined direction, on increasing the application of load, crack would become sufficiently inclined and start to extend upwards leading to immediate collapse of the bubbled slab in a flexural-shear failure mode with crushing of concrete near the point load, as shown in **Figs. 23, 26** and **32**.

5. SUMMARY AND CONCLUSIONS

The bubbled slabs with different PPR values had about (82% to 85%) of the failure load capacity of a similar reference solid slabs. The presence of plastic spheres voids used in the bubbled slabs increases the maximum crack widths and decreases the number of cracks in comparison with reference solid slab specimens.

Using prestressing steel in the bubbled slabs, increased the first cracking, the ultimate service and the failure loads. The increase of the first cracking load for bubbled slabs attained between (185.7% and 228%), while the increase of the failure load reached between (79.3% and 97.7%). Also, using prestressing steel in bubbled slabs resulted in a large decrease in the concrete compressive and tensile strains in comparison with non-prestressed bubbled slabs. There is a significant decrease in the maximum crack width and the number of cracks for bubbled slab with fully and partially prestressed reinforcement in comparison with non-prestressed bubbled slabs.

Increasing the partial prestressing ratio (PPR) to be (0.81) rather than (0.74) by increasing the number of strand from (2) to (3) in the bubbled slab, showed an increase in ultimate load by about (13.9%), a decrease in deflection at (0.7Pu) by about (21%), and an increase in the first cracking load by about (41.3%).

Increasing the diameter of plastic spheres used in bubbled slabs from (100mm) to (120mm) shows, a slight decrease in ultimate load about (3% to 7%), an increase in deflection at ($0.7P_u$) by about (0.5% to 29%) and a decrease the first cracking load by (14.2% to 25%).

REFERENCES

- ASTM Designation A416/A416M-2006, *Standard Specification for Steel Strand, Uncoated Seven-Wire for Prestressed Concrete*, ASTM International, Pennsylvania, United States.

- BUBBLEDECK, 2006, *Lighter Flat Slab Structures with BubbleDeck*, www.BubbleDeck-UK.com.

- BUBBLEDECK, 2006, *Technical Paper BubbleDeck Slab Properties, BubbleDeck Voided Flat Slab Solutions*, April, www.BubbleDeck-UK.com.

- BUBBLEDECK, 2006, *Test and Report Summary*, June, www.BubbleDeck-UK.com.

- Karayannis, C. G., and Chalioris S, C., 2013, *Design of Partially Prestressed Concrete Beams Based on the Cracking Control Provisions*, Engineering Structures Journal, Vol. 48, pp. 402-416.

- Marais, C. C., 2009, *Design Adjustment Factors and Economical Application of Concrete Flat Slabs with Internal Spherical Voids in South Africa*, M.Sc. Thesis, University of Pretoria.

- Naaman, A.E., 1992, *Unified Design Recommendations for Reinforced, Prestressed, and Partially Prestressed Concrete Bending and Compression Members*, ACI Structural Journal, pp. 200-210.

- Nielsen, M.P., 2004, *Technical Report from AEC Consulting Engineers Ltd*., The Technical University of Denmark.

- Salman, W.D., 2012, *Flexural Behavior of Bubbled Reinforced Concrete Slabs*, Ph.D. Thesis, University of Baghdad.

- Tan, K.G., Zhao, H., 2004, *Strengthening of Openings in One-Way Reinforced-Concrete Slabs Using Carbon Fiber-Reinforced Plastic Systems*, Journal of Composites for construction, ASCE, Vol. 8, No. 5, pp. 393-402.

NOMENCLATURE

A_{ps} = area of prestressing steel, mm^2

A_s = area of non-prestressed (ordinary) reinforcement, mm^2

f_{py} = yield strength of prestressing steel, MPa

f_y = yield strength of the ordinary reinforcement, MPa

Table 1. Characteristics of the Tested Slabs.

G	Specimen	Thickness of Specimen, mm	Number of Spheres	Sphere Diameter, mm	Distance c/c of Spheres, mm	D/H	Type of Reinforcement	Reinforcement in Tension Zone	PPR
1	S 1	150	0	-	-	-	Non-prestressed	2φ12 mm	0
	S 2						Partially Prestressed	2φ12 mm & 2φ12.7 mm	0.74
	S 3						Fully Prestressed	2φ12.7 mm	1
2	BD1	150	80	100	115	0.67	Non-prestressed	2φ12 mm	0
	BD2						Partially Prestressed	2φ12 mm & 2φ12.7 mm	0.74
	BD3						Fully Prestressed	2φ12.7 mm	1
	BD4						Partially Prestressed	6φ12 mm & 2φ12.7 mm	0.52
	BD5						Partially Prestressed	2φ12 mm & 3φ12.7 mm	0.81
	BD6						Fully Prestressed	3φ12.7 mm	1
3	BD7	150	48	120	145	0.80	Non-prestressed	2φ12 mm	0
	BD8						Partially Prestressed	2φ12 mm & 2φ12.7 mm	0.74
	BD9						Fully Prestressed	2φ12.7 mm	1

Table 2. Deflection at cracking, service and ultimate loads of tested specimens.

Specimen	Camber, (mm)	P_{cr}, (kN)	Δ_{cr}, (mm)	0.7 P_w, (kN)	Δ at 0.7P_w, (mm)	P_w, (kN)	Δ_w, (mm)
S 1	0	18	3.10	37.1	10.60	53	19.80
S 2	2.15	54	5.35	70.7	11.25	101	24.55
S 3	2.22	50	3.18	64.1	8.08	91.5	18.68
BD1	0	14	2.88	30.4	7.60	43.5	14.90
BD2	2.30	46	5.30	60.2	9.60	86	20.00
BD3	2.45	40	3.70	54.6	6.85	78	16.05
BD4	2.16	54	4.78	64.4	9.49	92	21.54
BD5	3.98	65	5.90	68.6	7.58	98	19.42
BD6	4.40	61	3.16	65.8	4.36	94	14.60
BD7	0	12	2.52	29.4	9.86	42	15.20
BD8	2.58	38	4.20	57.4	9.65	82	22.00
BD9	2.72	30	2.53	50.8	8.58	72.5	17.68

Table 3. Maximum crack width and failure mode of tested specimens.

Specimen	*Pcr*, (kN)	*Pu*, (kN)	*Pcr /Pu*	Maximum Crack Width, (mm)	Number of Crack	Mode of Failure	Shear Failure Angle, (degrees)
S 1	18	53	0.34	0.75	20	Flexure	-
S 2	54	101	0.53	0.21	11	Flexure	-
S 3	50	91.5	0.54	0.28	14	Shear	15.3
BD1	14	43.5	0.32	1.12	16	Flexure	-
BD2	46	86	0.53	0.27	10	Shear	10.3
BD3	40	78	0.51	0.30	12	Shear	13.4
BD4	54	92	0.58	0.21	8	Shear	10.20
BD5	65	98	0.66	0.22	8	Shear	17.0
BD6	61	94	0.64	0.26	9	Shear	15.5
BD7	12	42	0.28	1.67	13	Flexure	-
BD8	38	82	0.46	0.75	8	Shear	11.3
BD9	30	72.5	0.41	0.61	10	Shear	14.1

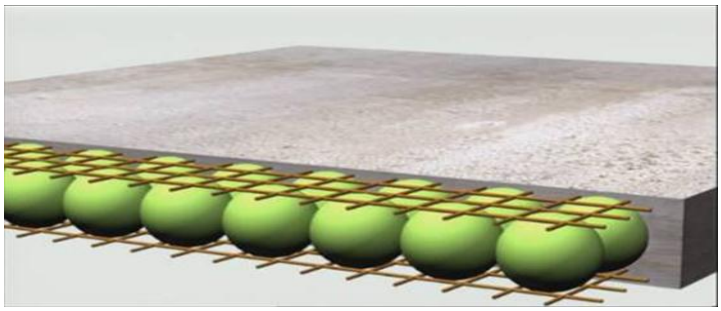

Figure 1. Bubbled Deck Floors System.

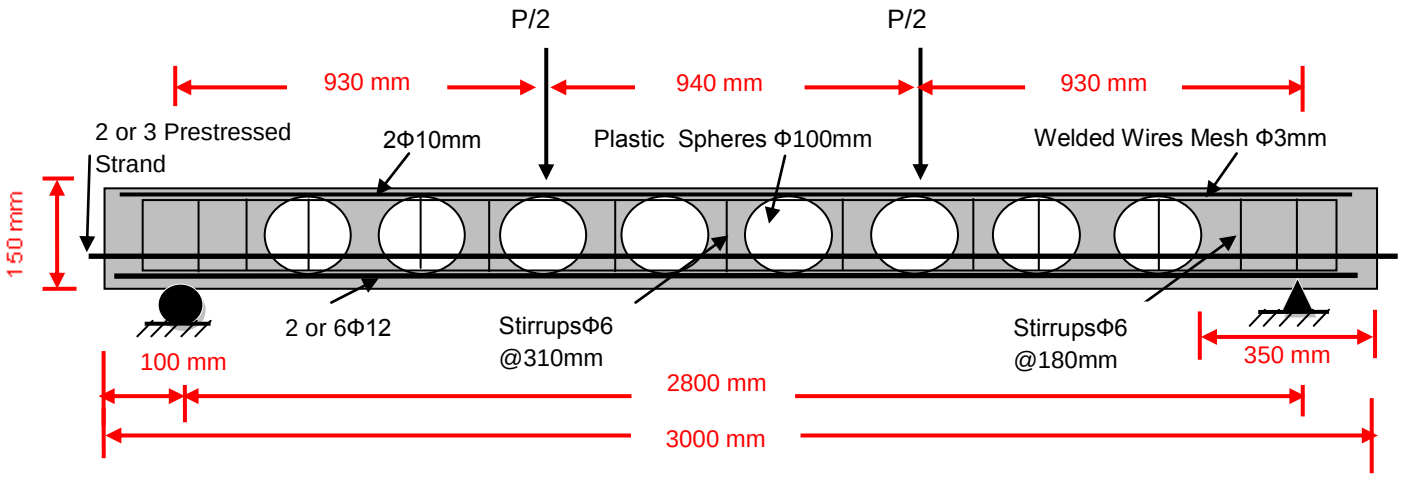

Figure 2. Bubbledeck Slab under Static Load.

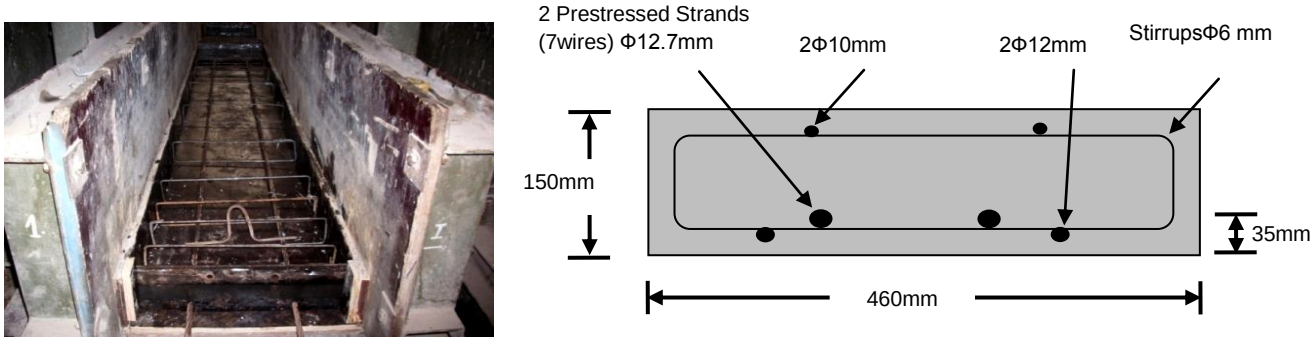

Figure 3. Reinforcement Details for Solid Slab of Group One.

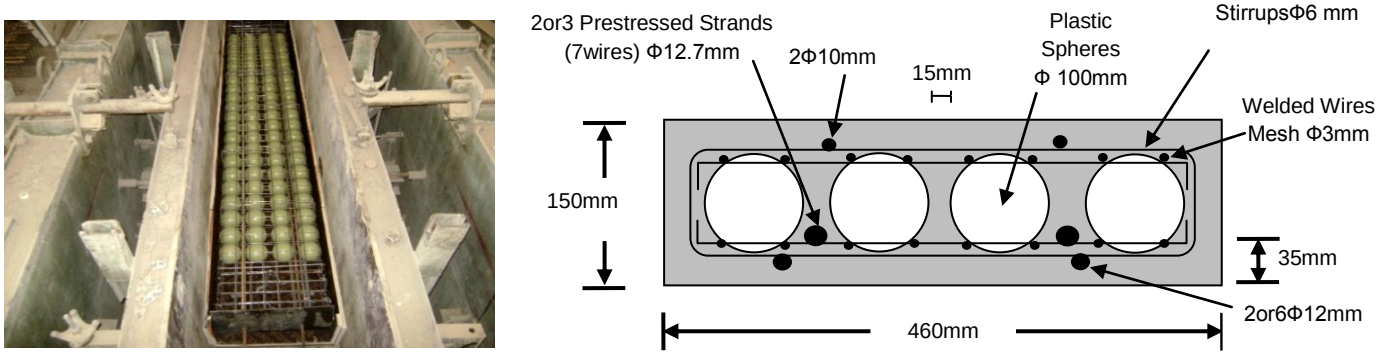

Figure 4. Reinforcement Details for Bubbled Slab of Group Two.

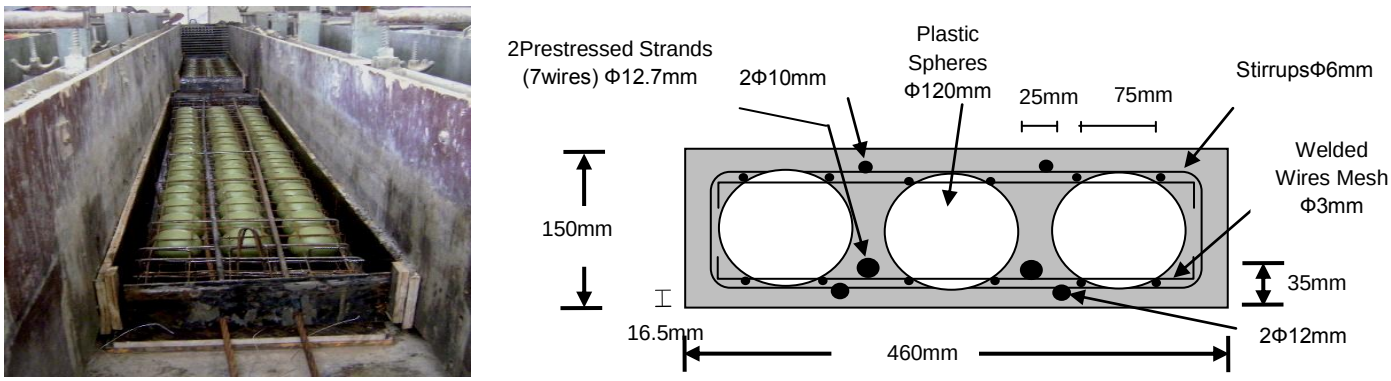

Figure 5. Reinforcement Details for Bubbled Slab of Group Three**.**

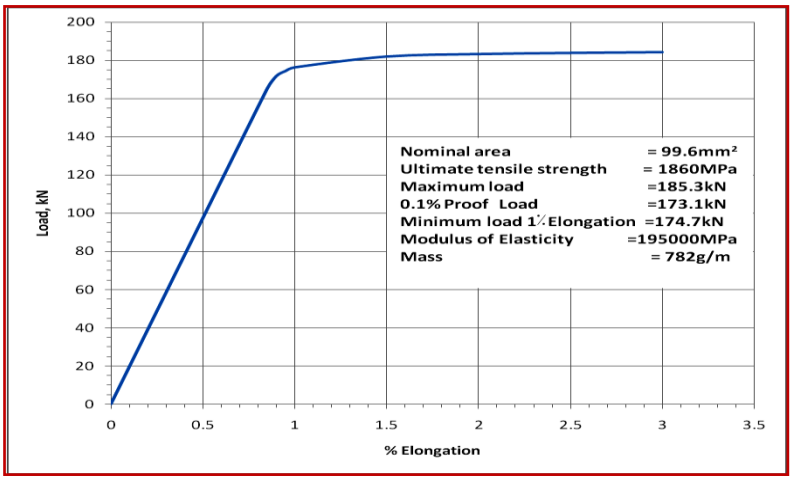

Figure 6. Load-Elongation Curve for (7wire) Strand (12.7mm) Diameter.

Figure 7. Preparation of Bubbled Slab Reinforcement.

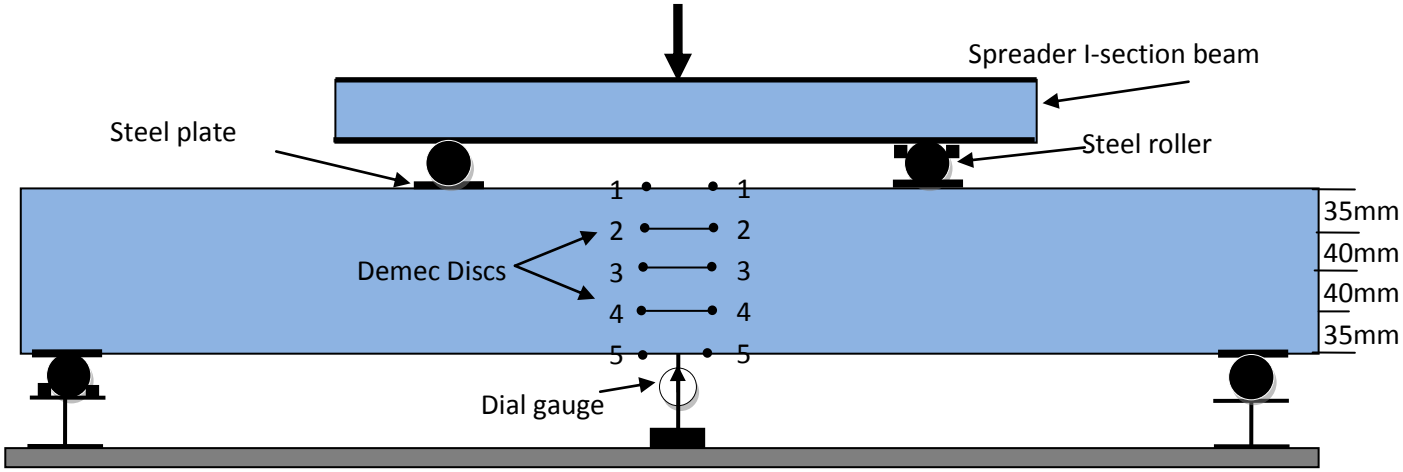

Figure 8. Arrangement of Dial Gauges and Demec Discs.

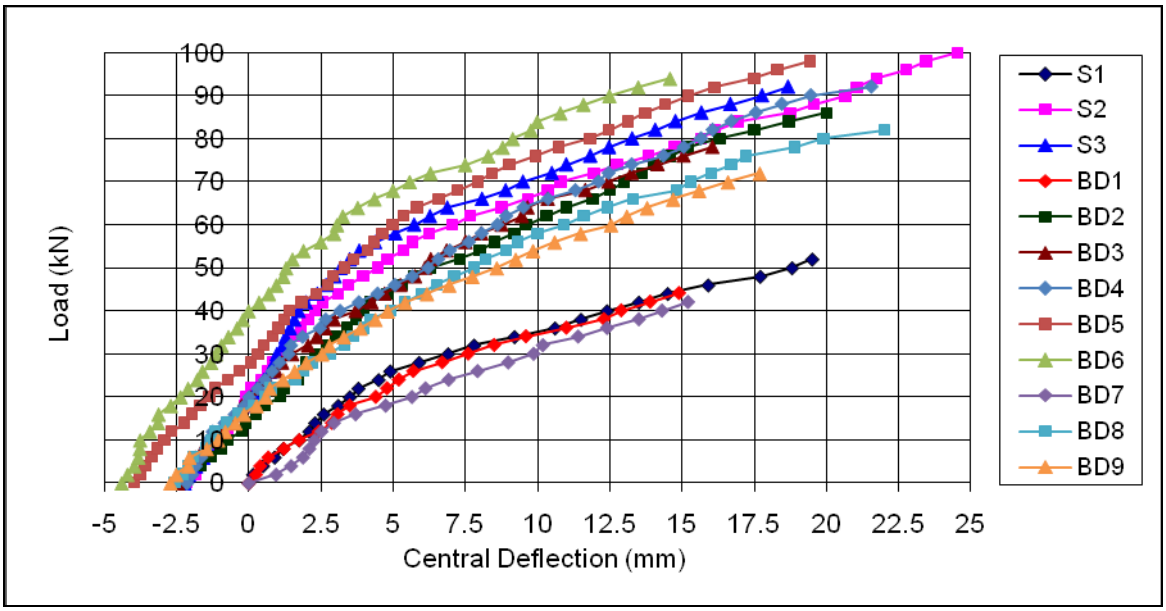

Figure 9. Load-Central Deflection Curve for Solid and Bubbled Slabs.

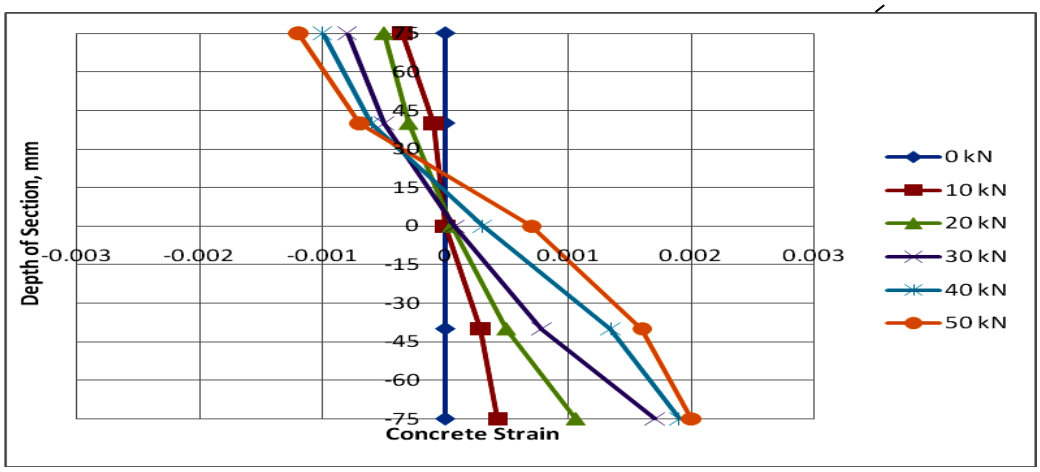

Figure 10. Load-Concrete Normal Strain Plot for Solid Slab S1.

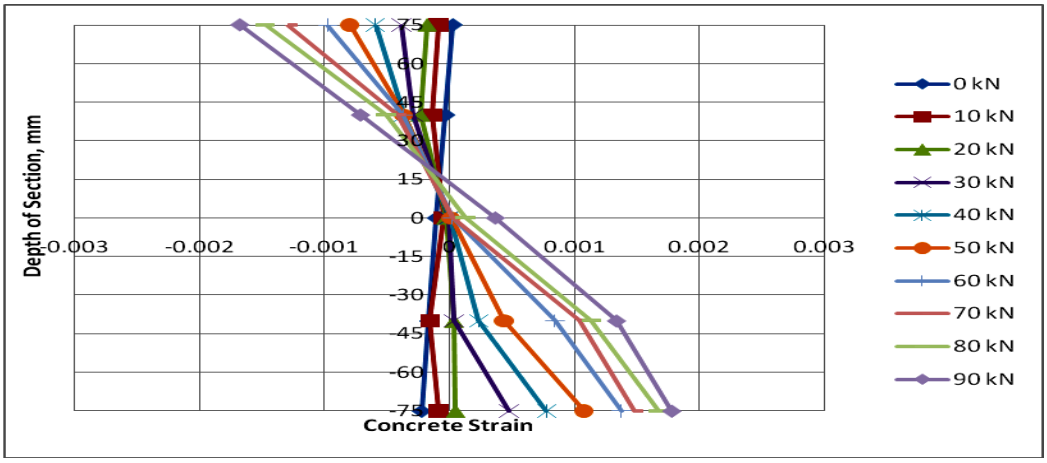

Figure 11. Load-Concrete Normal Strain Plot for Solid Slab S2.

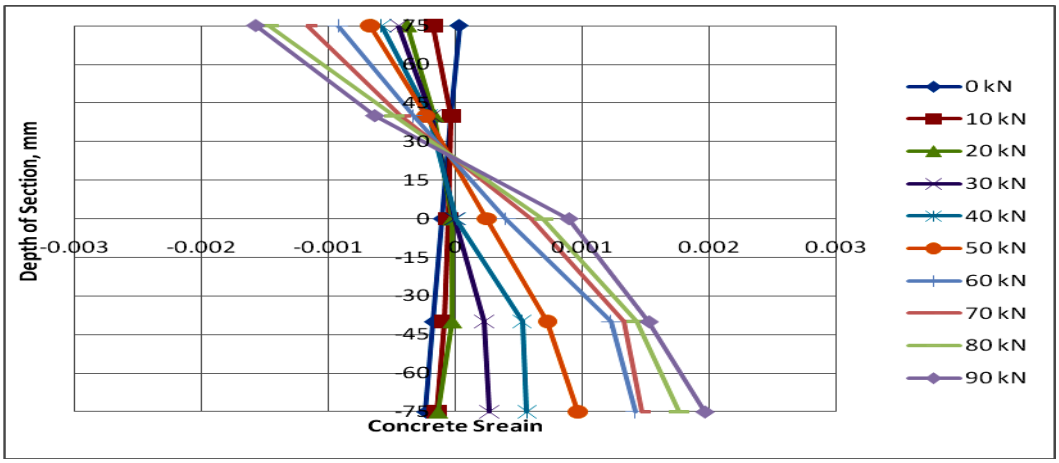

Figure 12. Load-Concrete Normal Strain Plot for Solid Slab S3.

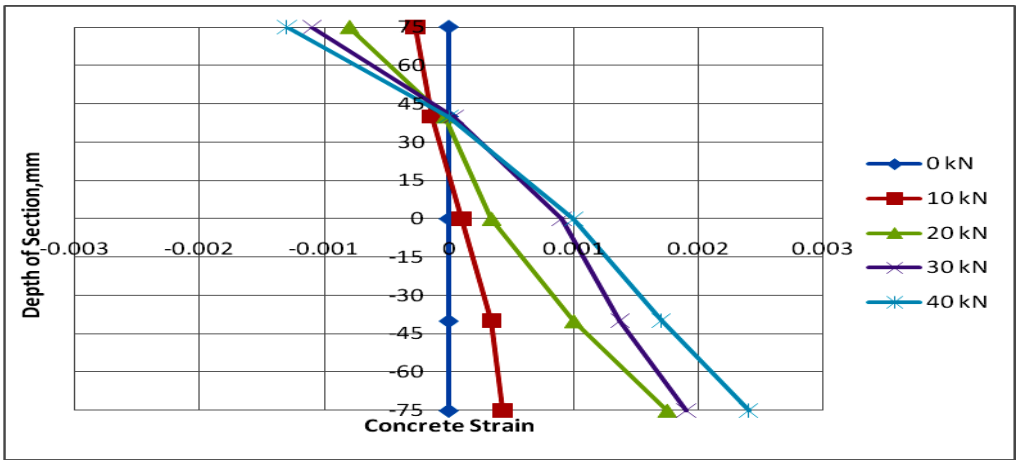

Figure 13. Load-Concrete Normal Strain Plot for Bubbled Slab BD1.

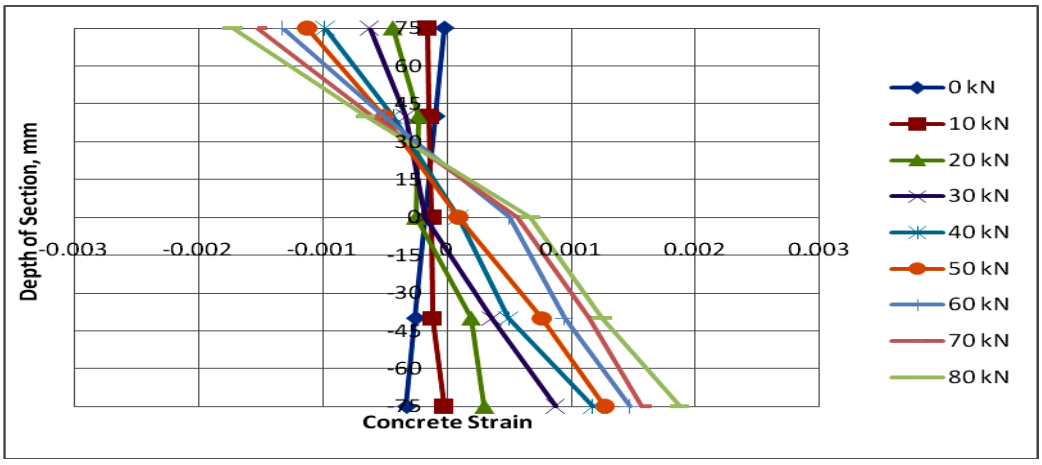

Figure 14. Load-Concrete Normal Strain Plot for Bubbled Slab BD2 **.**

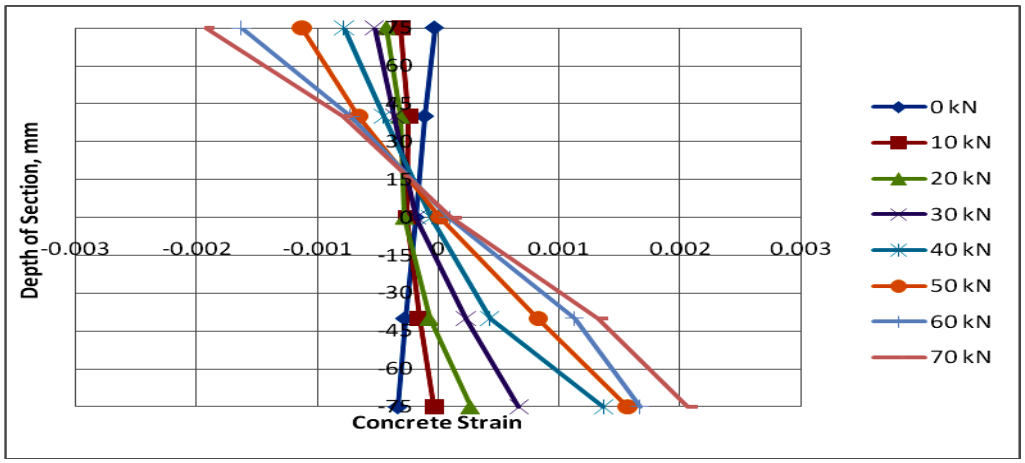

Figure 15. Load-Concrete Normal Strain Plot for Bubbled Slab BD3.

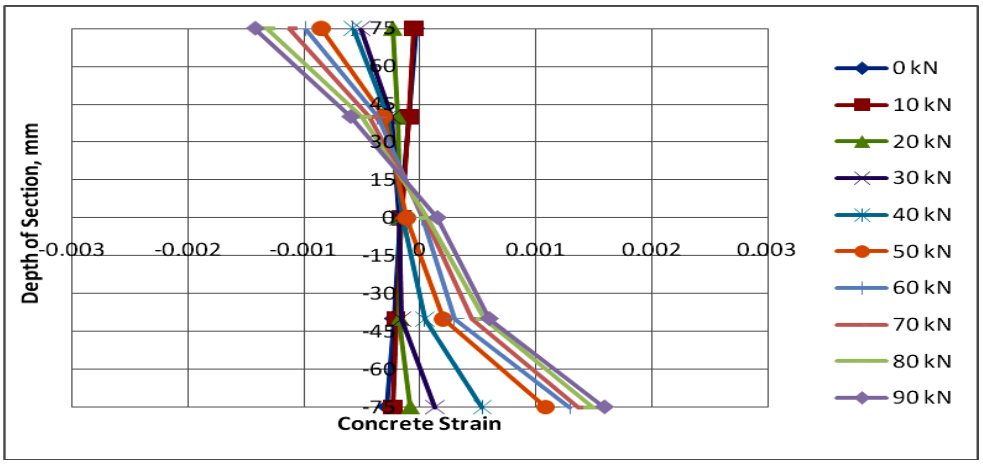

Figure 16. Load-Concrete Normal Strain Plot for Bubbled Slab BD4.

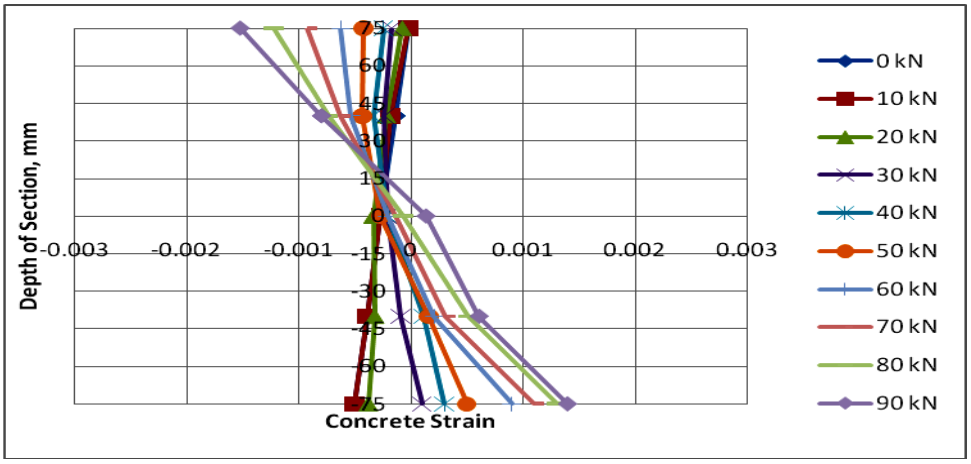

Figure 17. Load-Concrete Normal Strain Plot for Bubbled Slab BD5.

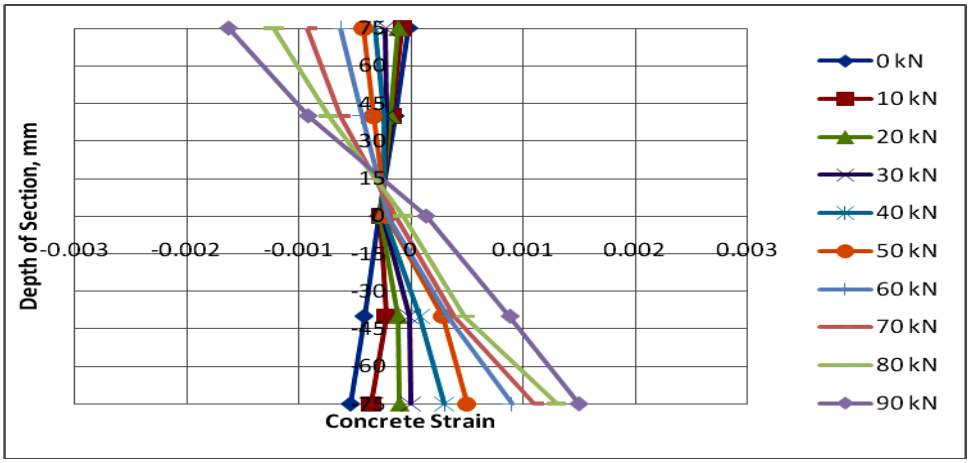

Figure 18. Load-Concrete Normal Strain Plot for Bubbled Slab BD6.

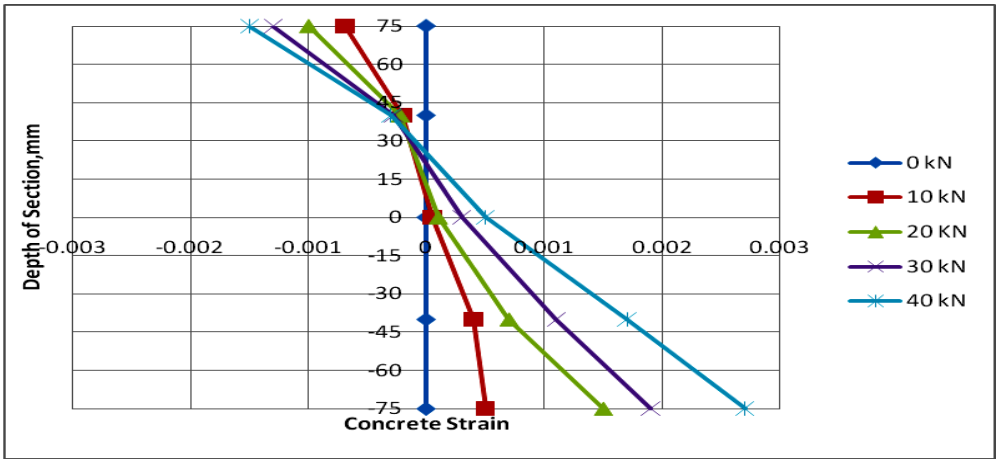

Figure 19. Load-Concrete Normal Strain Plot for Bubbled Slab BD7.

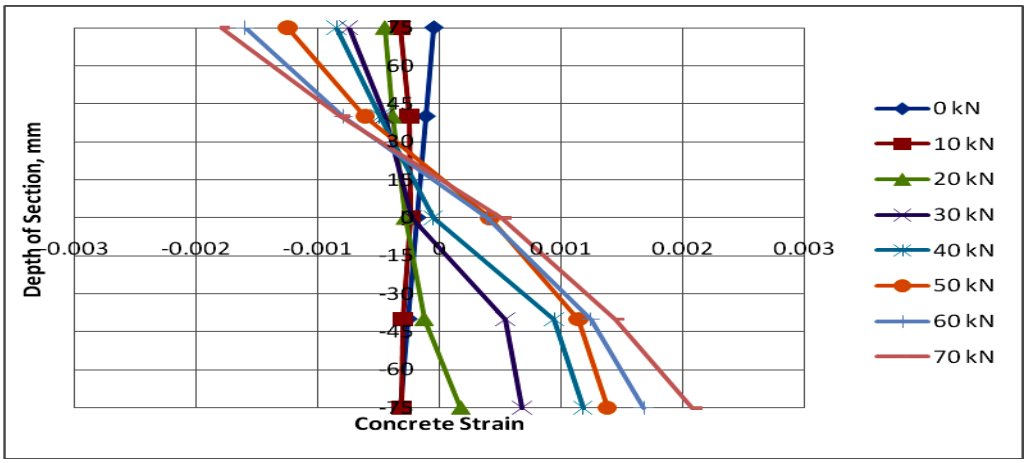

Figure 20. Load-Concrete Normal Strain Plot for Bubbled Slab BD8.

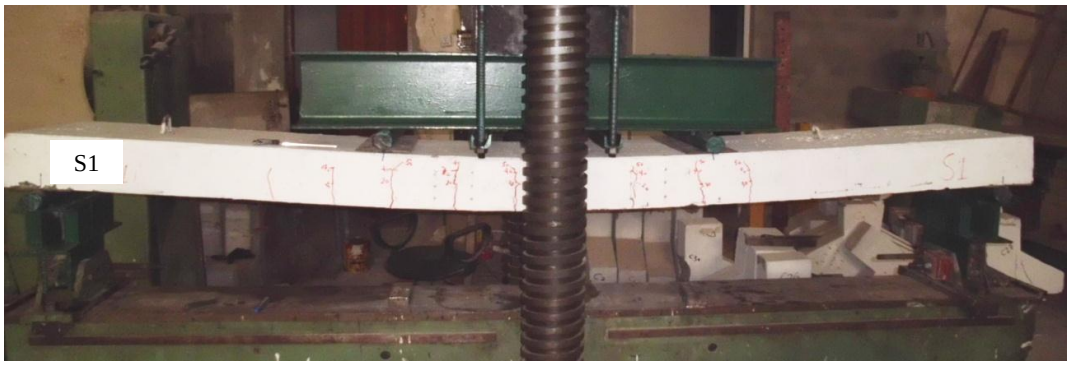

Figure 21. Crack Patterns and Failure Mode of Solid Slab (S1)**.**

Figure 22. Crack Patterns and Failure Mode of Solid Slab (S2)**.**

Figure 23. Crack Patterns and Failure Mode of Solid Slab (S3)**.**

Figure 24. Crack Patterns and Failure Mode of Solid Slab (BD1)**.**

Figure 25. Crack Patterns and Failure Mode of Solid Slab (BD2)**.**

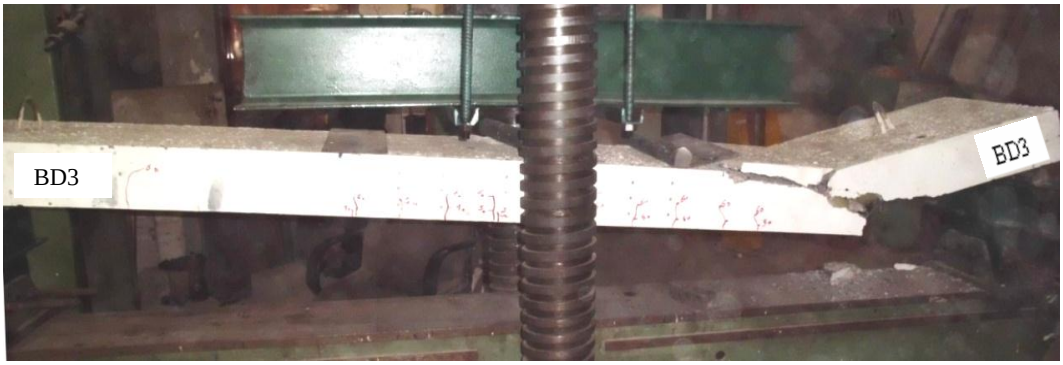

Figure 26. Crack Patterns and Failure Mode of Solid Slab (BD3)**.**

Figure 27. Crack Patterns and Failure Mode of Solid Slab (BD4)**.**

Figure 28. Crack Patterns and Failure Mode of Solid Slab (BD5)**.**

Figure 29. Crack Patterns and Failure Mode of Solid Slab (BD6)**.**

Figure 30. Crack Patterns and Failure Mode of Solid Slab (BD7)**.**

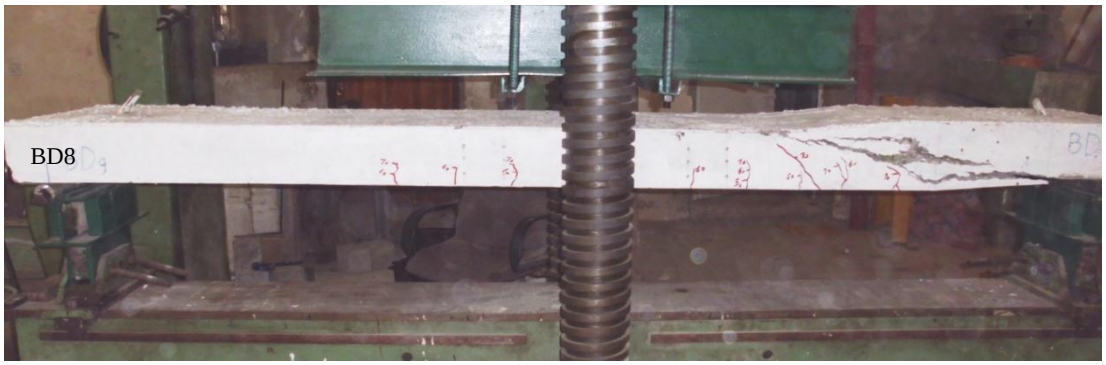

Figure 31. Crack Patterns and Failure Mode of Solid Slab (BD8)**.**

Figure 32. Crack Patterns and Failure Mode of Solid Slab (BD9)**.**